

Original Article

# Numerical Analysis of Consolidation Settlement of a Driven Square Concrete Pile in Soft Soil

Gbênihon Céleste-Amour Kenoukon<sup>1</sup>, Joseph Ng'ang'a Thuo<sup>2</sup>, Kiplagat Chehelgo<sup>2</sup>, Alphonse Ayado Owayo<sup>3</sup>

<sup>1</sup>Department of Civil and Construction Engineering, Pan African University Institute for Basic Sciences, Technology and Innovation (PAUSTI) Hosted at Jomo Kenyatta University of Agriculture and Technology, Nairobi, Kenya.

<sup>2</sup>Department of Civil Engineering, Dedan Kimathi University of Technology, Nyeri, Kenya.

<sup>3</sup>Department of Civil and Structural Engineering, Moi University, Eldoret, Kenya.

<sup>1</sup>Corresponding Author : [gbenihon.kenoukon@students.jkuat.ac.ke](mailto:gbenihon.kenoukon@students.jkuat.ac.ke)

Received: 04 March 2025

Revised: 05 April 2025

Accepted: 04 May 2025

Published: 31 May 2025

**Abstract** - This study investigates the consolidation settlement of a single pile by combining finite element modelling techniques and field data validation. Using Plaxis 2D and 3D, the study considers a series of static load tests performed over time on a pile driven in Florida and explores the performance of different modelling approaches. The pile is modelled with the soft soil advanced constitutive model, embedded beam row and soil volume. Two different geometry configurations are considered in the models. The average discrepancy between the numerical model values and the field measurement values is determined via the Mean Absolute Error (MAE) and the bias error. It was observed that the embedded beam row feature in the model has given satisfying results. The MAE is equal to 0.93, indicating a low discrepancy between the numerical model values and the reference values. Parametric investigations were conducted to explore soft clay parameters influencing displacement changes. Findings showed that the modified swelling index,  $\kappa^*$  is a critical parameter for the analysis, contributing 56% to the overall variation in the results. Cohesion and pile width also influenced, accounting for 22% and 13%, respectively.

**Keywords** - Consolidation, Driven pile, Finite element analysis, Settlement, Soft soil.

## 1. Introduction

Construction on soft ground areas presents considerable challenges in geotechnical engineering. The soft clay soils are intrinsically problematic due to their unique characteristics, such as high compressibility and water content, as well as low permeability. Consequently, consolidation settlement is predominant in these soils. This unfavorable behavior is largely attributed to the abundance of montmorillonite, a swelling clay mineral typically derived from basic and ultrabasic igneous parent rocks [1, 2]. In soft soils, structures often experience different damages, such as cracks, lateral movements, tilting, differential settlements, and collapse. Such deterioration may manifest within a few months of the construction's completion, progress insidiously over the years, or remain unnoticed until a critical failure develops. The associated maintenance and rehabilitation expenditures are estimated to run into billions of dollars annually [3, 4]. In soil profiles with deep, soft clay layers, shallow foundations' performance is insufficient to prevent large settlements [4, 5]. For instance, the "Leaning Towers of Santos" in Brazil, which fail to meet serviceability limit state requirements. Indeed, a combination of soft, compressible, clayey soil deposits and inadequate foundation design led to differential and excessive settlement of high-rise buildings. Close to a hundred buildings

tilt at scary angles in the city [6]. Maffei & Goncalves [6] presented in their work the plumb done for two buildings, Tower A and Tower B (each approximately 57 m tall) of the Condominium Nuncio Malzoni, with measured inclinations of 3.8% and 3.1% respectively.

To overcome the poor performance of shallow foundations, deep foundations, especially piles, have become the standard foundation solution for construction in soft soils [6, 7]. The need for a deep foundation in any project usually results from several factors, including subsurface conditions, foundation loads, and acceptable foundation settlement criteria [8, 9]. By transferring loads to competent strata at depth, piles markedly reduce superstructure movements and preserve serviceability [10]. However, excessive or any residual pile settlements can still compromise performance, making settlement control more important during design than the bearing capacity of the soil [11, 12]. To perform satisfactorily, foundations must have two main characteristics: they must remain stable against shear failure, and their post-construction settlement must stay within tolerable limits. Settlement prediction is a major concern and is a key design objective [13, 14].



The long-term behavior of piles is primarily caused by consolidation associated with the dissipation of installation-induced excess pore pressures. Since pile driving often occurs under undrained conditions in soft clay, significant excess pore water pressure will be generated in the soil due to the soil displacement. It results in larger settlement values and longer settlement stabilization time compared to bored piles [15-18]. In their statistical analysis of the long-term settlement of Piles in Shanghai Soft Clays, Wang et al. [18] showed that normalized settlements of precast-driven piles are roughly double those of bored piles and that stabilization occurs about two years later. In soft, clayey ground, even when the ultimate capacity of a pile foundation is met, the long-term settlement under sustained vertical static load remains critical [19-21]. As a case in point, the San Francisco Millennium Tower in the western United States is supported by a reinforced concrete slab constructed over 900 piles driven into marine clay. The expected settlement was around 300 mm over its lifetime [22]. But since its completion, the building has been settling and has reached, on average, a value of 400 mm in 2020 [23]. Tilting has also been noticed towards the northwest direction, as shown in Figure 1 [22]. This case highlights the need for advanced numerical models to accurately predict pile consolidation settlement in clay soils. Investigating the consolidation settlement for structures is essential because excessive settlements may create severe safety issues [20, 24, 25].

The problems related to foundations in soft soils exist from field investigation to their modelling behavior [26]. The Finite Element Method (FEM) is a widely adopted numerical tool in civil engineering. It is employed both for research studies and practical design of engineering problems [26, 27]. The complex behavior of soils can be modelled with more advanced constitutive soil models. The soil's nonlinearity with plastic deformations and the stress path can be more easily captured. The FEM is especially effective in depicting deformation modes and stress distribution throughout loading up to failure [28, 29].

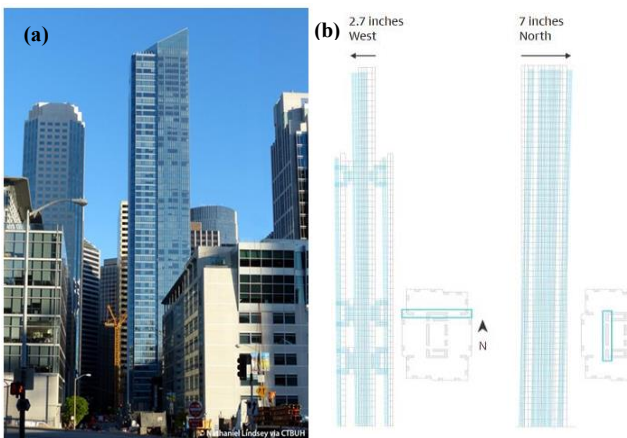


Fig. 1(a) Millennium Tower in San Francisco, and (b) Tilting of the tower in Northwest Direction [22].

Sun et al. [30] studied the sensitivity of the influencing factors of single-pile stability through a three-dimensional finite element simulation model. The results provided valuable insights, namely the main factors affecting the pile stability, such as the elastic modulus, Poisson's ratio, friction coefficient, and the angle of internal friction. Despite this, using a Mohr-Coulomb elastic-plastic model for soil doesn't allow the explicit modelling of the consolidation settlement in clay soils. The study considered multiple soil layers, such as sand, fine clay, coarse gravel, strongly weathered monzonite, and medium-weathered monzonite. Moreover, the sensitivity analysis lacks parameters specific to consolidation behavior.

Additionally, Wang et al. [31] examined the long-term differential settlement of piled rafts and their influence on building shortening. The model predicts a pot-shaped settlement distribution (higher settlement in the core) for piled rafts. A time-dependent soil-foundation-structure system with equivalent springs is then developed to predict the vertical shortening of shear walls and mega columns. The model uses an empirical equation with parameters calibrated by finite element analysis. While this approach is beneficial for computational simplicity, it may not fully capture the nonlinear consolidation behavior of the soil.

Using the case history of the Messeturm tower founded on a piled raft in Frankfurt, Germany, Franzen & Reul [7] conducted a detailed numerical back analysis with a three-dimensional finite element model. The nonlinear behavior of the overconsolidated Frankfurt Clay was simulated with a hypoplastic material law. The model allows for time-dependent effects analysis. In line with this, Ganai & Reul [32] employed a visco-hypoplastic material model to capture the time-dependent material behavior of the Frankfurt clay. The numerical simulation of the SGZ-Bank building, founded on a raft foundation, was presented and compared to the measurements taken. The viscosity index, which controls creep deformations, was found to have almost no influence on the raft foundation settlement at the time of completion. Moreover, different viscosity indices lead to different settlement rates in the first years after completion, but the effect decreases with time [32].

On the other hand, Franzen & Reul [7] identified that an increase in the viscosity index results in an increase in creep settlement over 40 years. However, these modelling studies focused on the analysis of piled rafts and raft foundations in overconsolidated clays with specific stiffness properties. The variations in the hypoplastic model regarding the critical compressibility properties in soft clays were poorly examined.

The reviewed studies have achieved worthwhile findings in predicting settlement in soft clay soils through numerical analysis. Nevertheless, the consolidation behavior of a driven single pile and the influence of the parameters governing it remains insufficiently explored.

This work intends to bridge this gap by employing both two-dimensional and three-dimensional finite element models with Plaxis software. For that purpose, the well-documented case study of the driven piles in Florida was used [33, 34]. The field instrumentation included static load tests performed over time under realistic loading scenarios, making it a rare and valuable dataset for numerical models. Based on the results of the Dilatometer Test (DMT) and Cone Penetration Test (CPT), the material behavior of the site soil has been modelled with the soft soil model, which allows us to account for consolidation effects.

## 2. Methodology

### 2.1. Description of the Case Study

The research of McVay et al. [33] investigates the behavior of five full-scale 457 mm square prestressed concrete piles over time. Instruments were fixed on the piles, which were then driven at active bridge construction sites owned by the Florida Department of Transportation (FDOT) in northern Florida. Many static tests were performed using an Osterberg cell (O-cell) cast into the pile bottom, as shown in Figure 2. Strain gages, DMT cells and piezometers were also installed along the pile. Two methods were used to monitor the pile top movement during the static load tests. Measurements were obtained using both a wireline and a survey level. These two measurements agreed well for all of the tests. In this paper, the pile of interest is the pile driven at the Vilano Bridge north of the west abutment. The site of Vilano West (VLW) has a primary soil type ranging from Soft to medium-stiff silty clay. Preliminary CPT and DMT soundings were performed, as shown in Figures 3 and 4. The pile was dynamically tested to estimate static capacity using a Pile Driving Analyzer during initial driving and short-term set checks. The shaft resistance and end bearing estimated during restrrike are respectively 465 kN and 422 kN.

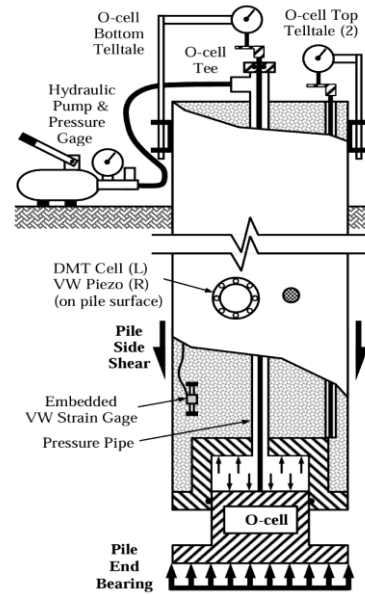


Fig. 2 Pile and Instrumentation used for static load test [33]

### 2.2. Numerical Modelling

#### 2.2.1. General Considerations

The finite element analyses were carried out with Plaxis software in both two-dimensional (2D) and three-dimensional (3D) configurations. The pile was modelled as plane strain. The model size and the meshing significantly impact how the detailed stress-strain response and deformations are captured. To avoid model disturbances due to too-close boundaries, a sensitivity analysis was done, and two geometries were used to evaluate the influence of domain size and mesh refinement on the results.

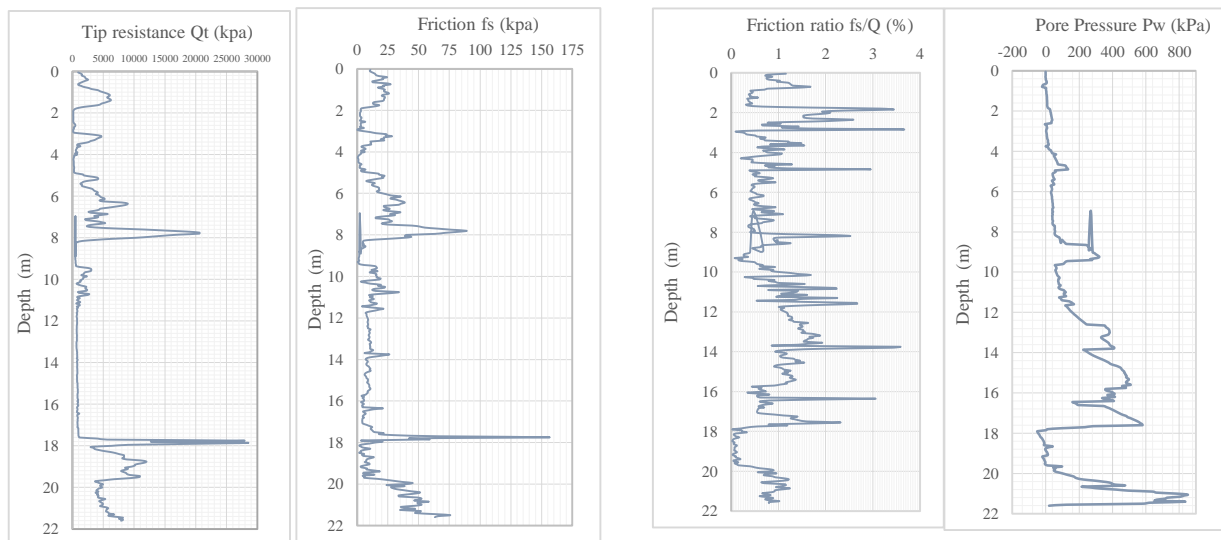


Fig. 3 CPT Sounding at Vilano West site [34]

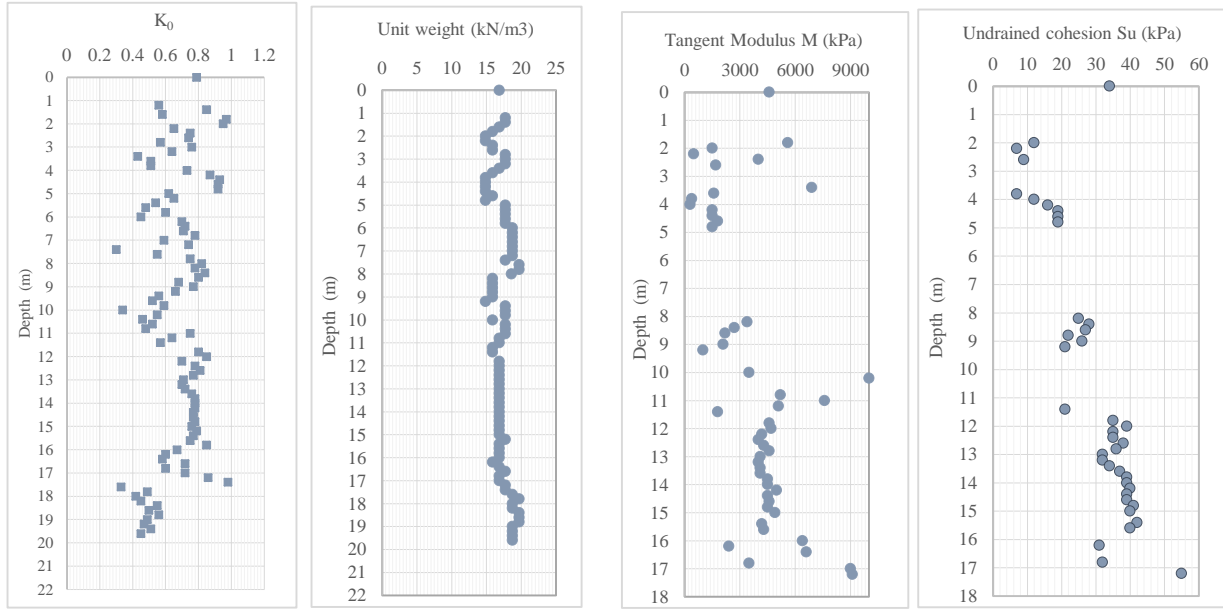


Fig. 4 DMT results from Vilano West site [34]

### 2.2.2. Geometry

To ensure a comprehensive evaluation of the pile behavior in soft soil, two different geometries were used for the numerical simulations. Model 1: a  $20 \times 22 \text{ m}$  model size ( $20 \times 20 \times 22 \text{ m}$  in 3D) and a larger Model 2:  $40 \times 40 \text{ m}$  ( $40 \times 40 \times 40 \text{ m}$  in 3D), in Figures 5 and 6. The geometry of model 1 was chosen based on the CPT soil profile data, which indicated that a smaller domain would be sufficient to capture the pile's settlement behavior under the given soil conditions.

### 2.2.3. Pile Model

Pile-soil interaction being intrinsically a three-dimensional phenomenon. Conventional models in two dimensions are unable to capture it fully. To mitigate this shortcoming, the embedded beam row feature represented the pile. Accurately modelling pile-soil response is challenging. The traditional method with plate elements or discrete node-to-node anchors idealization to approximate the pile is subject to notable limitations. The embedded beam row provides more realistic pile-soil interaction behavior compared to other methods. The beam element with the pile behavior option can interact and connect with soil with special interface elements (shaft and base resistance). It has been validated by many studies [35-38]. In the 3D model, the square pile of 18.5 m in length was modelled using a volume element with positive interface elements embedded within a 3D soil volume. The linear elastic behavior was assumed due to the high stiffness of the pile material relative to the surrounding soil.

### 2.2.4. Boundary Condition

The pile was centrally positioned, ensuring sufficient distance to minimize boundary effects. Boundary conditions were applied to simulate realistic constraints. The model is

assumed to be fully fixed at the bottom of the mesh and normally fixed for the vertical boundaries.

### 2.2.5. Mesh Generation

To optimize computational efficiency, a global mesh coarseness factor of 0.70 was applied for model 1, ensuring a balance between accuracy and computational time. In contrast, the model 2 ( $40 \times 40 \text{ m}$ ) domain, which was larger, was used to assess the impact of domain size on the numerical results, particularly regarding boundary effects. For this case, the mesh was refined within a 5 m radius from the pile. This was done to account for areas of high stress and displacement concentration around the pile shaft and surrounding soil (Figure 6). Refining the mesh in these critical regions where there are high stresses and displacement concentration improves the accuracy of the results by capturing localized soil-pile interactions more effectively. For all the soil elements, 15-noded tetrahedral elements were used for meshing. The 15-node triangular element utilizes fourth-order displacement interpolation and evaluates stresses at 12 integration points, offering high computational accuracy [36]. A fine mesh is generated for the whole model to optimize the convergence.

### 2.2.6. Constitutive Model

For the simulation of the behavior of the soil, the Soft Soil (SS) model was used. Unlike the Mohr-Coulomb material model, the soft soil model is a more advanced constitutive material model and is more suitable for saturated soft soils, where significant nonlinearity is expected. It can represent both elastic and plastic material states and is used for highly compressible soil. It also takes account of the memory for pre-consolidation stress [39-41]. The SS model uses effective stress-based formulations, essential for modelling accurate

simulation of consolidation processes and excess pore water pressure dissipation around the pile due to loading. As shown in Figure 7, the failure condition in the SS model can be described by a Mohr-Coulomb failure line. However, the volumetric hardening is predicted and expressed in terms of the modified compression index,  $\lambda^*$  and modified swelling index  $\kappa^*$ . These indices account for the high compressibility of soft soil, providing a realistic representation of how the soil deforms under loading conditions [42].

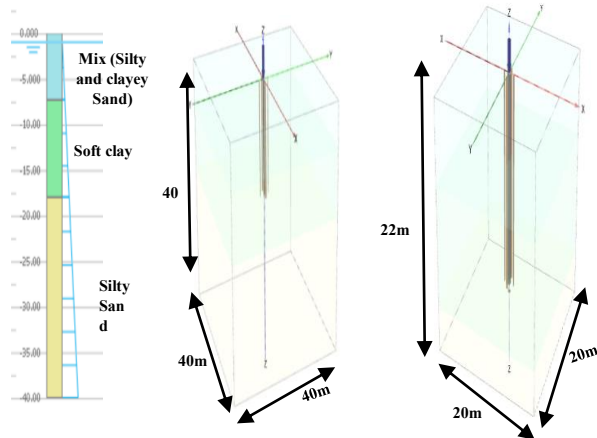


Fig. 5 Pile in the 3D geometry models with interface elements

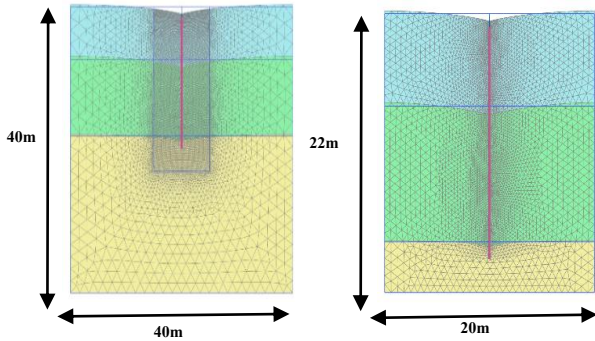


Fig. 6 Deformed mesh of the pile in the 2D geometry models

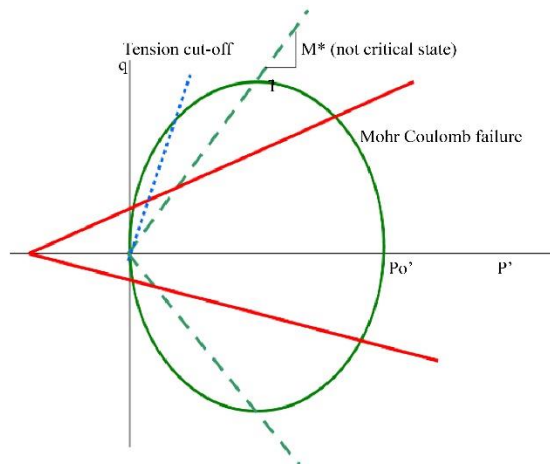


Fig. 7 Soft soil model [41]

Table 1. Model input parameters

|                                       | Soil 1                | Soil 2    | Soil 3     | Pile                              |
|---------------------------------------|-----------------------|-----------|------------|-----------------------------------|
| Type                                  | Silty and clayey sand | Soft clay | Silty sand | Embedded beam row/ volume element |
| Model                                 | Soft soil             |           |            | Elastic                           |
| Type of drainage                      | Undrained A           |           |            |                                   |
| $\gamma_{unsat}$ (kN/m <sup>3</sup> ) | 16                    | 15        | 17         | –                                 |
| $\gamma_{sat}$ (kN/m <sup>3</sup> )   | 16.97                 | 17.11     | 19.10      | –                                 |
| $e_0$                                 | 1.28                  | 1.25      | 0.74       | –                                 |
| $c'$ (kPa)                            | 20                    | 30        | 15         | –                                 |
| $\phi'$ (°)                           | 38                    | 25        | 40         | –                                 |
| $\lambda^*$                           | 0.065                 | 0.081     | 0.037      | –                                 |
| $\kappa^*$                            | 0.005                 | 0.01      | 0.005      | –                                 |
| POP (kPa)                             | 58.76                 | 76.3      | 82.2       | –                                 |
| $K_0$                                 | 0.69                  | 0.68      | 0.5        | –                                 |
| $R_{inter}$                           | 0.9                   | 0.8       | 0.9        |                                   |
| $E$ (kPa)                             | –                     | –         | –          | 30.68 *10 <sup>6</sup>            |
| $F_{max}$ (kN)                        | –                     | –         | –          | 422                               |
| $T_{skin}$ (kN/m)                     | –                     | –         | –          | 60                                |

### 2.2.7. Materials Properties

The soil conditions correspond to a coastal plain area. A soft clay is found along the bottom half of the pile (10.7 m), topped by a mix of silty and clayey sand over 7.3 m. The soil stratigraphy was generated by the borehole from the field CPT data with a groundwater level of -0.89 m. A notable amount of ground investigation data is available from the McVay et al. [34] database.

The SS model parameters have been deduced from these test results. For each layer, the average representative means values of the parameters have been chosen (See Table 1). The soil unit weight from the dilatometer test was used to calculate the void ratio. The relationship for saturated soils is given by Equation (1) [43].

$$e = \frac{G_s \gamma_w - \gamma}{\gamma - \gamma_w} \quad (1)$$

Where,  $G_s$  = specific gravity of solids,  $\gamma$  the soil bulk unit weight,  $\gamma_w$  = unit weight of water ( $9.81 \text{ kN/m}^3$ ). Based on the material models manual of Plaxis [41], the modified compression and swelling index was estimated using Equation (2), and the ratio  $\lambda^*/\kappa^*$  assumed to be equal to 3. The plasticity index  $I_p$  was calculated from the friction ratio of the CPT results. The over-consolidation ratio  $OCR$  and the pre-consolidation stress  $\sigma_p$  are directly taken from the DMT results available in the case study report [34]. Equations (3) and (4) from [41] were used to deduce the pre-overburden pressure  $POP$  value. The pile elastic modulus value was calculated by back analysis of the applied load versus strain data during testing. The value is reported in the study report [34]. The skin resistance and base resistance of the embedded beam row element are derived from the dynamic testing of the driven precast pile. The CAPWAP (Case Pile Wave Analysis Program) was used to estimate the resistance distribution along the shaft and toe of the pile. The values, testing and calculation details are mentioned in the case study reports [33, 34].

$$\lambda^* = I_p(\%)/500 \tag{2}$$

$$OCR = \sigma_p/\sigma'_y \tag{3}$$

$$POP = |\sigma_p - \sigma'_y| \tag{4}$$

Where  $I_p$  is the plasticity index,  $\sigma_p$  the pre-consolidation stress and  $\sigma'_y$  the in-situ effective vertical stress.

### 2.2.8. Construction Stages for the Static Load Test Modelling

To be able to represent adequately the field conditions, the calculation steps of the model were divided into nine (9) construction stages. This allows for agreement with the pile construction, monitoring and testing. The initial stress distribution was calculated with  $K_0$  analysis in the initial phase.

The procedure was adopted because the surrounding terrain is essentially level around the pile, eliminating potential equilibrium issues at the initialization stage. The second stage considered the pile installation. As the authors have mentioned, only single drops of the ram were required to drive the pile due to the soil's relatively low resistance. The pile installation is just modelled by activating the embedded beam row material in the 2D model and the soil volume in the 3D.

In the following phases, consolidation analysis was performed with adequate time intervals, considering the time at which the static tests were carried out. The time corresponds to the elapsed time after the completion of pile driving. Each consolidation phase was followed by a plastic analysis to calculate the pile settlement under the maximum sustained load at the time. A plastic analysis was considered as the load was applied for only 4 min during the testing [33]. The load values and corresponding times are shown in Table 2.

Table 2. Load test modelling stages

| Stage             | Calculation type | Duration (day) | Applied load (kN) |
|-------------------|------------------|----------------|-------------------|
| Initial Phase     | $K_0$ analysis   | -              | -                 |
| Pile installation | Plastic          | -              | -                 |
| Phase 2           | Consolidation    | 0.26           | -                 |
| Phase 3           | Plastic          | -              | 469               |
| Phase 4           | Consolidation    | 2.58           | -                 |
| Phase 5           | Plastic          | -              | 581               |
| Phase 6           | Consolidation    | 16.13          | -                 |
| Phase 7           | Plastic          | -              | 697               |
| Phase 8           | Consolidation    | 138            | -                 |
| Phase 9           | Plastic          | -              | 845               |

## 3. Results and Analysis

### 3.1. Static Load Test Modelling

The first part of the analysis investigates the different models' abilities to reproduce the real measurements in situ. The results of the models (see Figures 8-11) are then compared to the field measurements, as shown in Figure 12.

Just a few hours after the pile driving, the significant changes in the axial force (an increase of respectively 23.88%, 48.61% and 80.17%) were also reflected in the settlement. As underlined by many authors such as Hosseini and Rayhani [44] and Jiang et al. [45], the increase of driven pile capacity with time is mainly due to the dissipation of excess pore water pressure generated around the pile during driving. The consolidation and ageing of the disturbed soil near the pile are also subsequent factors. Consequently, this affects the pile settlement evolution, which tends to increase with time as the soil adjacent to the pile shaft reconsolidates and becomes progressively stable. This trend can be observed in the field measurement where the maximum settlement starts from 6.35 mm on the first day and reaches 8.38 mm on the second, 3.63 mm and 6.48 mm, respectively, on 18.98 and 157 days. The pattern is, moreover, consistent with the results of Zhao et al. [17].

The error metrics between the predicted values and the reference values were calculated using the Mean Absolute Error (MAE) given by Equation (5):

$$MAE = \frac{1}{n} \sum_{i=1}^n |Predicted_i - Reference_i| \tag{5}$$

MAE represents the average absolute difference between predicted and reference values, providing a general measure of prediction accuracy. The Bias errors given by Equation (6) were also used to identify underprediction or overprediction trends. It provides the average deviation between the predicted and reference values, showing whether predictions tend to

overestimate (positive bias) or underestimate (negative bias) [46-48].

$$Bias = \frac{1}{n} \sum_{i=1}^n (Predicted_i - Reference_i) \quad (6)$$

The 2D model 2 has the lowest errors. The average discrepancy between the numerical model values and the reference values is MAE = 0.93, indicating the most accurate prediction. The average difference between maximum settlement values is 7%, indicating a high reliability of the data obtained with this model. The performance of this model configuration can be attributed to the inherent advantages of the embedded beam row feature in Plaxis 2D, as discussed in previous literature [35, 37, 38, 49-52]. A key factor might also be the combination of sufficient domain size and mesh refinement in critical areas near the pile. The embedded beam row in the 2D model simplifies the interface behavior while

maintaining sufficient accuracy. It incorporates line-to-line spring-slider interface elements that capture localized stress and displacement concentrations. It is associated with a mesh continuity, unlike other elements that introduce artificial discontinuities. Mesh distortion and dependency are avoided due to its superimposed beam structure with the soil mesh. Additionally, the larger domain effectively minimizes boundary effects that could otherwise distort the results. In contrast, the discrepancy in the 3D model with full-volume element representation can be attributed to the numerical complexities, resulting in some limitations.

The bias errors calculated showed negative values for all cases, as presented in Figure 13. This indicates that the numerical models have an overall under-prediction trend. This observation could be attributed to the assumptions made in the constitutive model, which may underestimate certain soil behaviors, such as localized plastic deformations.

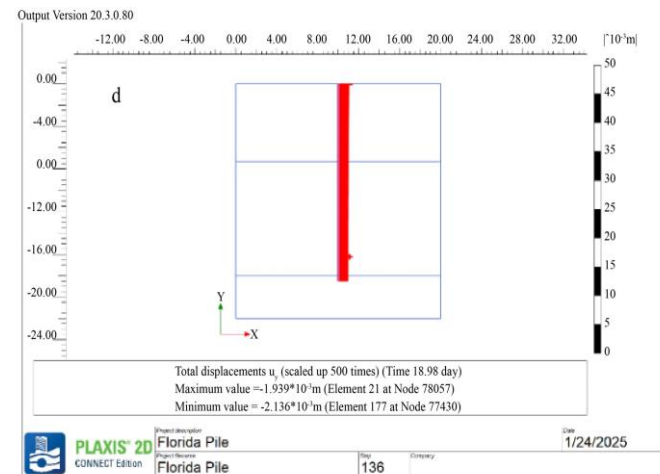
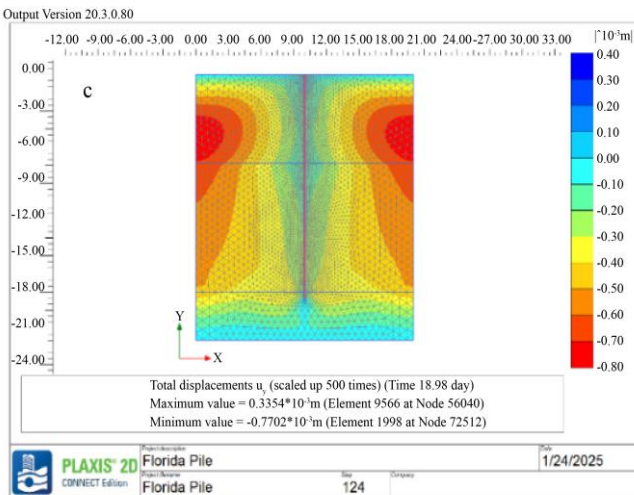
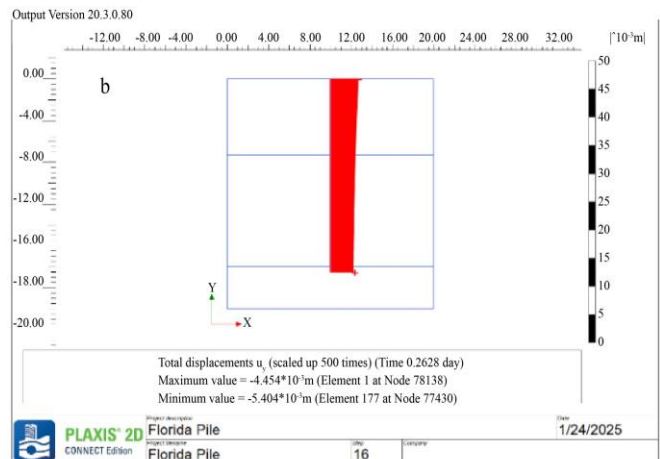
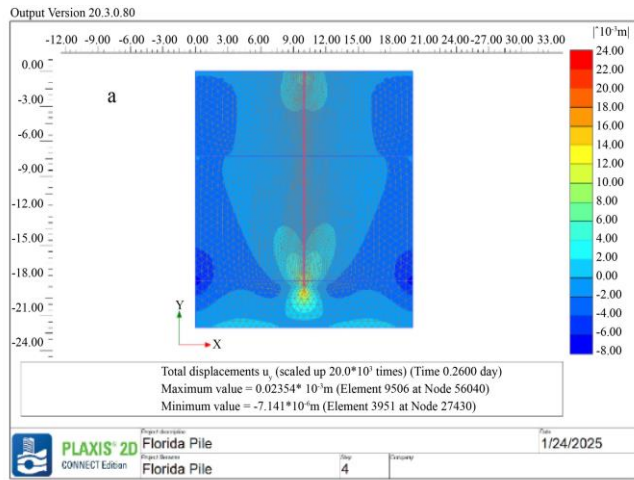


Fig. 8 Total displacement  $u_x$  in 2D for model 1: (a) consolidation analysis contours of displacement at 0.26-day, (b) Pile settlement distribution at 0.26-day, (c) consolidation analysis contours of displacement at 18.98 days, and (d) Pile settlement distribution at 18.98 days.

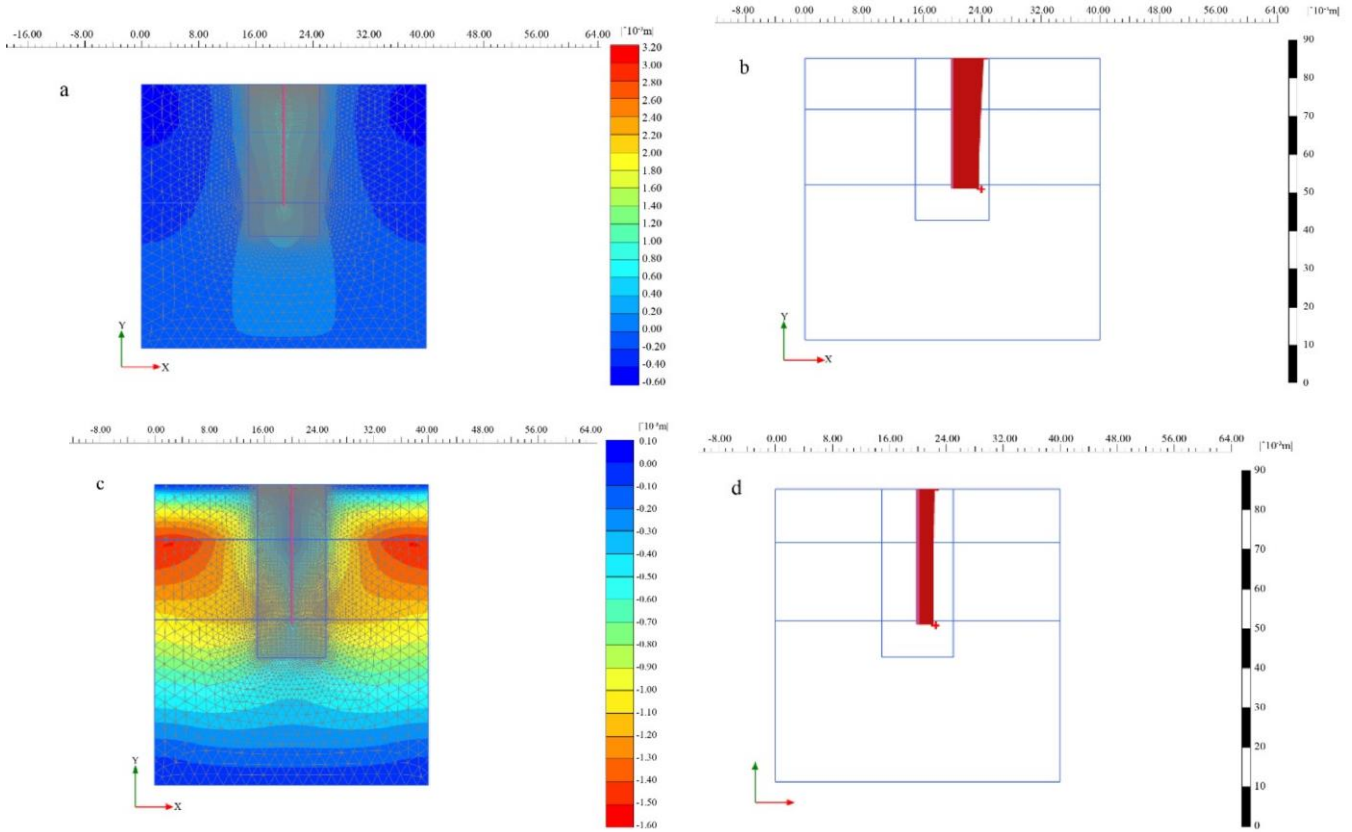


Fig. 9 Total displacement  $u_x$  in 2D for model 2: (a) consolidation analysis contours of displacement at 2.84 days, (b) Pile settlement distribution at 2.84 days, (c) consolidation analysis contours of displacement at 157 days, and (d) Pile settlement distribution at 157 days.

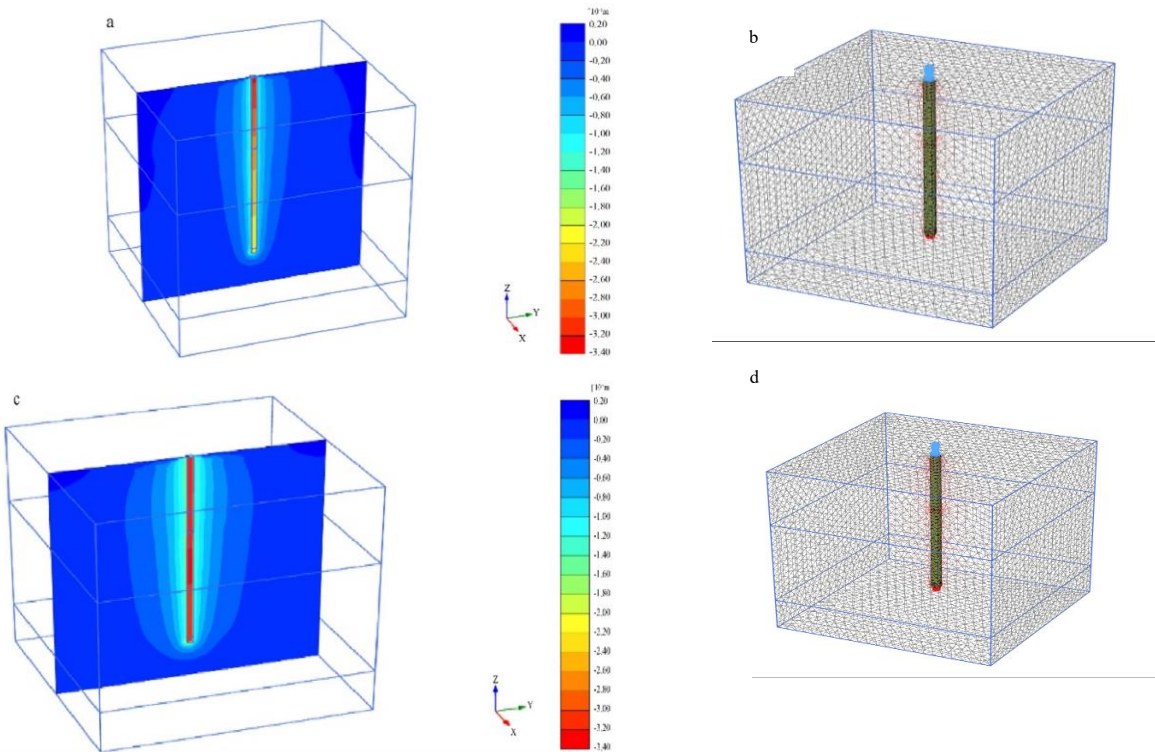


Fig. 10 Total displacement  $u_z$  in 3D for model 1: (a) cross-section of consolidation analysis at 18.98 days, (b) Pile settlement distribution at 18.98 days, (c) cross-section of consolidation analysis at 157 days, and (d) Pile settlement distribution at 157 days.

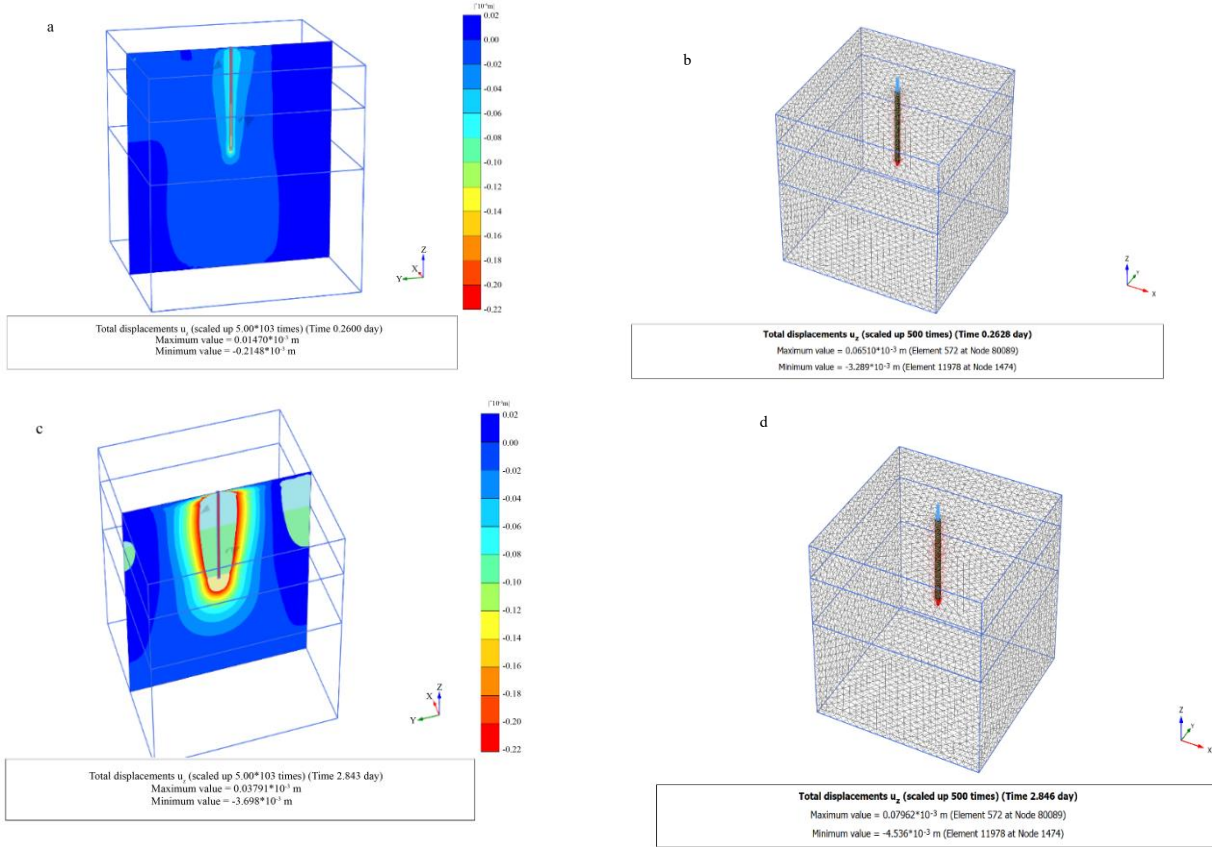


Fig. 11 Total displacement  $u_z$  in 3D for model 2: (a) cross-section of consolidation analysis at 0.26-day, (b) Pile settlement distribution at 0.26-day, (c) cross-section of consolidation analysis at 2.84 days, and (d) Pile settlement distribution at 2.84 days.

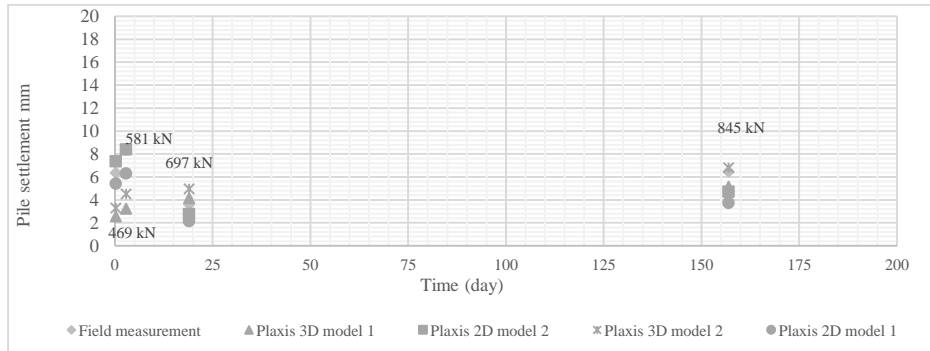


Fig. 12 Field measurements vs Plaxis models results at maximum load over time

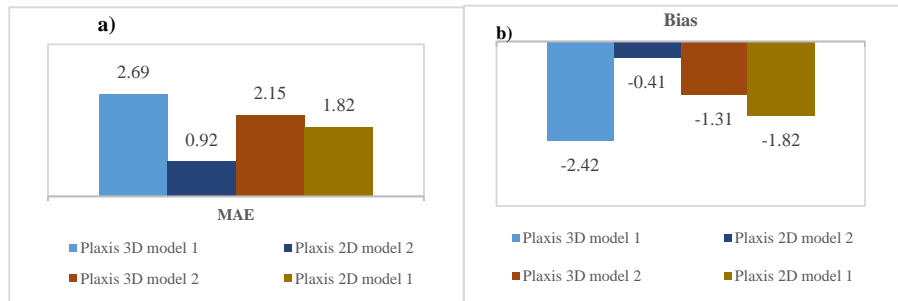


Fig. 13 Error values of the numerical modelling

**3.2. Modelling of the Pile behavior under Permanent Load and Sensitivity Analysis**

The pile was modelled under different loading ranges over time to assess the evolution of the settlement. The 2D model 2 was used for its best performance in reproducing the field behavior.

In-depth analyses were then conducted to evaluate the settlement sensitivity to the soft clay soil parameters in the model. The construction stages used for the analysis are shown in Table 3.

Consolidation analysis was performed by successively increasing the overload on the pile from 300 kN to 1000 kN. The load application time varies from 150 days to 1000 days, and the reached time at the end of the analysis (phase 6) is 2000 days. The sensitivity analysis starts by calculating the SensiScore, which indicates how much a selected parameter influences the pile settlement. The most significant parameters are presented in Table 4.

Figure 14 shows that the pile settlement evolves continuously, presenting a time-dependent settlement behavior. This trend of the settlement has been mentioned in the works of [31, 45, 53]. It can be seen in Figure 14(a) that a greater value of  $\kappa^*$  makes the settlement increase more rapidly than a lower value.

At day 150, the settlement is 6.12 mm for  $\kappa^* = 0.008$  but reaches a value of 8.89 mm when  $\kappa^* = 0.02$ . At day 2000, the settlement value is 31.72 mm for  $\kappa^* = 0.008$  and 40.45 mm for  $\kappa^* = 0.02$ .

This sensitivity is due to the control of this parameter over soil deformation under reloading. A higher  $\kappa^*$  indicates increased soil compressibility, which accelerates settlement, particularly in soft soils where consolidation is time-dependent.

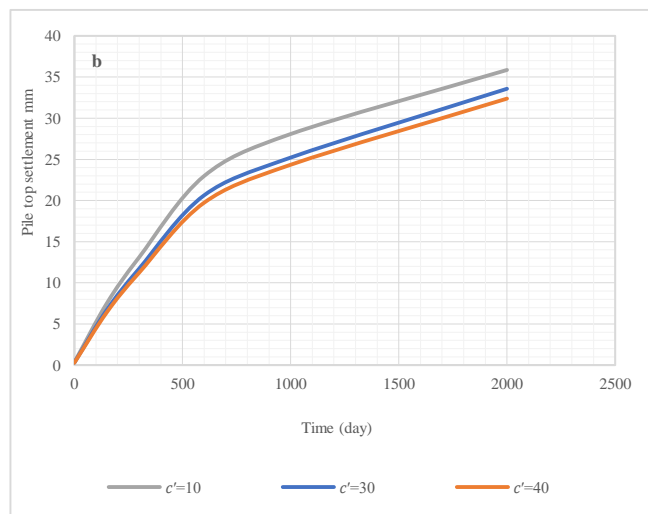
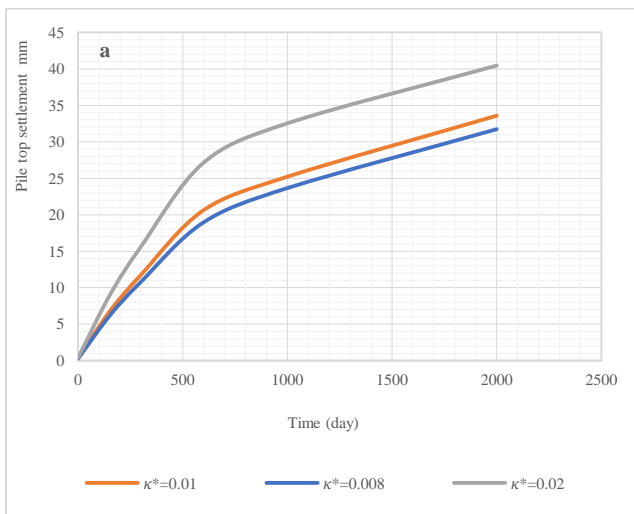
**Table 3. Modelling stages for sensitivity analysis**

| Stage             | Calculation type | Applied load (kN) | Time at the end of the stage (day) |
|-------------------|------------------|-------------------|------------------------------------|
| Initial Phase     | $K_0$ analysis   | -                 | -                                  |
| Pile installation | Plastic          | -                 | -                                  |
| Phase 2           | Consolidation    | 300               | 150                                |
| Phase 3           |                  | 500               | 300                                |
| Phase 4           |                  | 800               | 600                                |
| Phase 5           |                  | 900               | 1000                               |
| Phase 6           |                  | 1000              | 2000                               |

**Table 4. Parameters range of values**

| Parameters | Min   | Max  | SensiScore |
|------------|-------|------|------------|
| $\kappa^*$ | 0.008 | 0.02 | 56         |
| $c'$       | 10    | 40   | 22         |
| $\varphi'$ | 20    | 30   | 9          |
| Width $d$  | 0.3   | 0.5  | 13         |

Moreover, Figure 14(b) highlights that with a lower value of  $c'$ , the pile settles more with time. The settlement value reaches 35.86 mm at day 2000 for  $c' = 10 kPa$ , but 32.38 mm for  $c' = 40 kPa$ . Which corresponds to a diminution of 9.7% for a higher cohesion value. However, in Figure 14(c), it can be seen a slightly faster settlement with  $\varphi' = 30^\circ$  than  $\varphi' = 20^\circ$ . In Figure 14(d), it was observed that pile settlement increased with a decrease in pile width. For a lower value of  $d = 0.3 m$ , the settlement is slightly higher, 34.85 mm at 2000 days, but equal to 33.67 mm for  $d = 0.5 m$ .



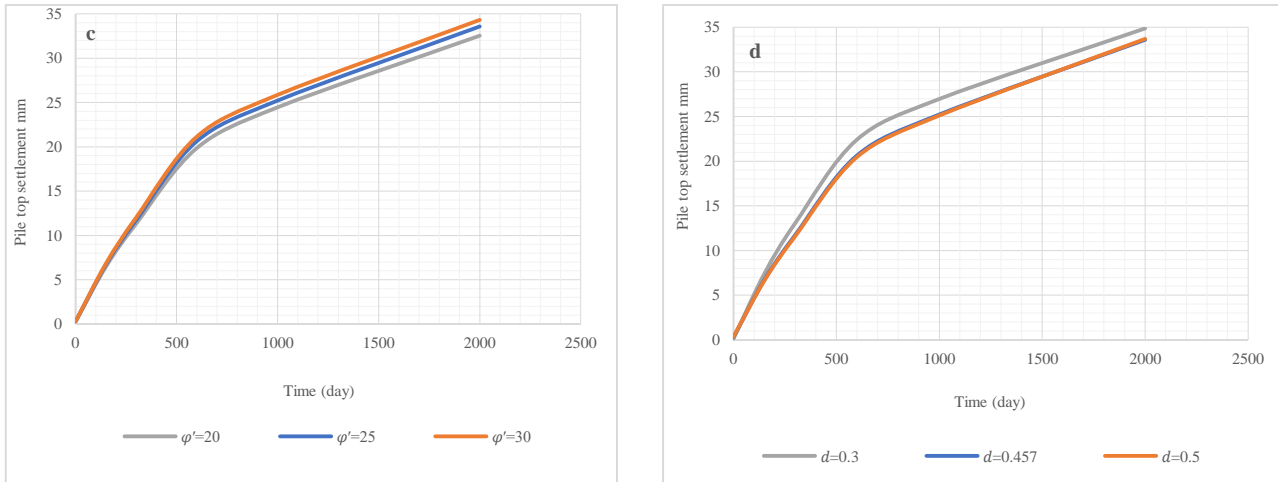


Fig. 14 Evolution of Pile settlement over time: (a) Influence of  $\kappa^*$ , (b) Influence of  $c'$ , (c) Influence of  $\phi'$ , and (d) Influence of  $d$ .

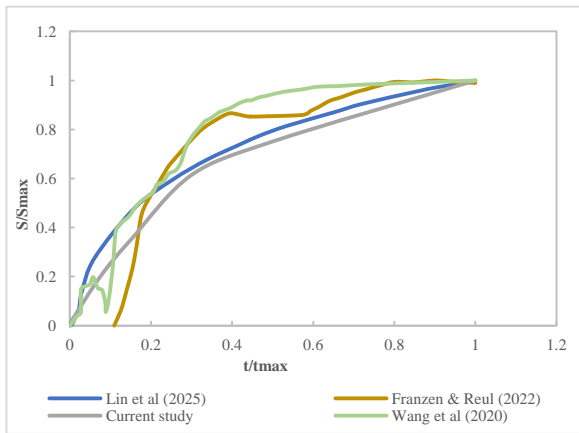


Fig. 15 Normalized time-settlement curves of the current study vs previous studies

#### 4. Discussion

The settlement of piles presents different variations over time depending on the soil behavior. Therefore, depending on the soil model and its parameters. Lin et al. [54], in their modelling of pile-supported embankments in deep soft soil, used the soft soil creep model. The study highlighted the sensitivity of the settlement to the modified compression index  $\lambda^*$ , swelling index  $\kappa^*$ , and modified creep index  $\mu^*$ . It was pointed out that the impacts of these parameters on the deformation of soft soil are significant and complex. The influence of the strength parameters  $c$  and  $\phi$  of soft layers to pile displacement was mentioned by Wang et al. [55]. A suite of numerical simulations revealed that the cohesion and the internal friction angle of the soft strata are dominant controlling parameters. A higher value of these parameters was linked to reducing the maximum deformation. According to Xu et al. [56], the contribution of  $\phi'$  tends to be more predominant when the loading reaches three times the design bearing load. Vardanega [57] has also concluded the contribution of those parameters. His study shows that a pile found in strata with a stronger cohesion profile can carry a

higher load, leading to a smaller settlement. In addition, the pile diameter affects the pile's bearing capacity and ability to resist settlement. A larger diameter increases the contact area between the pile and the surrounding soil, reducing settlement for a given load. Figure 15 shows the normalized time-settlement responses obtained from this current numerical modelling and previous studies. The normalized curves help to reveal trends in the rate and extent of consolidation independently of scale differences. It showcases the consistency and variability inherent in pile performance over time. The curves presented distinctive consolidation settlement behaviors with both similarities and deviations. These differences underscore the influence of varying soil models, parameters and loading conditions. The differences primarily appear at early and intermediate times, which denote the construction process and early structural response dissimilarities.

The model of Lin et al. [54] based on soft soil creep, highlighting the creep effect, presents a curve aligned with the current study. Both of the curves predict similar settlement trends and rates. In general, they show notably gradual consolidation behaviors to the maximum settlement. Moreover, a relatively moderate and consistent settlement rate was achieved in their initial responses. Approximately 70% of the maximum settlement was reached at  $t/t_{max} = 0.4$ , compared to nearly 90% for Wang et al. [31] and Franzen & Reul [7]. The model of the latter exhibits much steeper initial responses. Despite the compressibility of the soft clay layers in the current study ( $\kappa^* = 0.01$ ) and in the study by Lin et al. [54] ( $\kappa^* = 0.0127$  and  $\kappa^* = 0.0068$ ), the distribution observed for these studies can be explained by the presence of different soil layers with varying  $\kappa^*$ . Lin et al.'s [54] moderate consolidation rate can also be attributed to their specific construction methodology. A methodology that involved staged surcharge preloading followed by long-term

embankment loading, resulting in an extended primary consolidation phase. However, the Soft Soil Creep Model with relatively balanced  $\kappa^*$  values (0.0068-0.0184) produced more pronounced settlement in the middle time range compared to the current study. The model's explicit creep component amplifies the effect of the  $\kappa^*$  values.

The homogeneous overconsolidated Frankfurt Clay soil condition with a single  $\kappa^*$  value in Franzen & Reul's [7] model appears to facilitate rapid initial settlement. It suggests that uniform soil conditions may promote consistent consolidation rates early in the loading process. Incorporating rate-dependent deformation in Mašin's hypoplastic model [7] can also explain the intensification of the consolidation response, whether the rapid initial response or the continued settlement development after the main consolidation phase. The fluctuations of the groundwater level and the combined loading effect of the massive structure (1860 MN) also considerably influence the modelling. These factors contrast with the current study considerations, namely the stable groundwater conditions and the smaller loads applied. The model of Wang et al. [31] also presents rapid settlement progression. It is characterized by a fast attainment of high percentages of the maximum settlement. The normalized curve of the model shows irregular settlement behavior in the early stages, displayed by fluctuations. Such behavior reflects the complex soil-structure interactions in their super-tall building scenario. It might also suggest sensitivity to differential settlement effects influenced by structural stiffness and loading variations during the construction phase. Over the longer term, the settlement curve converges smoothly. It demonstrates stabilization as the primary consolidation is complete, and differential effects diminish under a balanced structural load. This tendency can be explained by the Hardening Soil Model used, which emphasizes stress-dependent stiffness rather than time effects.

## References

- [1] Hamzah Abd. Hamid et al., "Prediction of Soil Settlement on Soft Clay Soil Using Normalized Rotational Multiple Yield Surface Framework (Nrmysf)," *Journal of Technology*, vol. 85, no. 1, pp. 43-51, 2022. [[CrossRef](#)] [[Google Scholar](#)] [[Publisher Link](#)]
- [2] N.O. Mohamad et al., "Challenges in Construction Over Soft Soil - Case Studies in Malaysia," *IOP Conference Series: Materials Science and Engineering: Soft Soil Engineering International Conference*, Langkawi, Malaysia, vol. 136, no. 1, pp. 1-8, 2016. [[CrossRef](#)] [[Google Scholar](#)] [[Publisher Link](#)]
- [3] Ali Akbar Firoozi, Ali Asghar Firoozi, and Mojtaba Shojaei Baghini, "A Review of Clayey Soils," *Asian Journal of Applied Sciences*, vol. 4, no. 6, pp. 1319-1330, 2016. [[Google Scholar](#)] [[Publisher Link](#)]
- [4] Vivek Kumbhare et al., "Experimental Studies on Alternate Foundations for Load Transfer in Deep Clay Deposits," *Materials Today: Proceedings*, vol. 73, no. 1, pp. 167-179, 2023. [[CrossRef](#)] [[Google Scholar](#)] [[Publisher Link](#)]
- [5] A.C. Cattell, "Shallow Foundation Problems and Ground Conditions in Torbay," *Read at the Annual Conference of the Ussher Society*, vol. 10, pp. 68-71, 2000. [[Google Scholar](#)] [[Publisher Link](#)]
- [6] Carlos E.M. Maffei, and Heloisa H.S. Gonçalves, "Innovative Techniques Used to Plumb Two 57 m Height Concrete Buildings Leaning 3.8 and 3.1 %," *Innovative Infrastructure Solutions*, vol. 1, pp. 1-18, 2016. [[CrossRef](#)] [[Google Scholar](#)] [[Publisher Link](#)]
- [7] Aljoscha Franzen, and Oliver Reul, "Numerical Investigation of the Long-Term Settlement Behaviour of Piled Rafts in Over-Consolidated Clay," *20<sup>th</sup> International Conference on Soil Mechanics and Geotechnical Engineering*, Sydney, pp. 1-7, 2022. [[Google Scholar](#)] [[Publisher Link](#)]

## 5. Conclusion

This study investigated the behavior of a driven pile foundation in soft ground, subjected to external loads and soil consolidation. Numerical analyses of the foundation were achieved using Plaxis 2D and 3D. The results demonstrated the capability of numerical modelling, particularly when performed with suitable geometry size, mesh refinement and efficient approaches, to predict the pile settlement. A good correlation between the static load test model and the observed field measurements was observed at 0.26, 2.84, 16.98 and 157 days. A comprehensive sensitivity analysis was conducted to identify the key parameters influencing pile settlement over time. The vertical displacements of the foundation were investigated throughout 2000 days. Consolidation analysis was realized with overloads of 300 kN, 500 kN, 800 kN, 900 kN and 1000 kN. The results indicated that the modified swelling index  $\kappa^*$ , cohesion  $c'$ , friction angle  $\phi'$  and pile width are notable factors affecting the rate and magnitude of settlement. An increase of  $\kappa^*$  the significantly accelerated settlement, reflecting the impact of soil compressibility on time-dependent behavior. Lower values of  $c'$  led to increased settlement, demonstrating the critical role of soil shear strength in resisting deformation. The effects of the friction angle  $\phi'$  and pile width  $d$  were found to be secondary, with relatively minor variations in settlement observed.

## Funding Statement

The authors express their appreciation to the African Union Commission for their financial backing, which supported the research and the publication of this work.

## Acknowledgements

The authors thank the Pan African University Institute for Basic Sciences, Technology, and Innovation for the research environment and the various presentations that improved this work.

- [8] Rolf Katzenbach, Steffen Leppla, and Deepankar Choudhury, *Foundation Systems for High-Rise Structures*, 1<sup>st</sup> ed., CRC Press, pp. 1-314, 2016. [[CrossRef](#)] [[Google Scholar](#)] [[Publisher Link](#)]
- [9] Mohshin Ali et al., “Numerical Analysis of Soil–Pile Interface Properties of Bored Pile Embedded in Silty Clay Soils,” *BAIUST Academic Journal*, vol. 4, no. 1, pp. 1-13, 2023. [[Google Scholar](#)] [[Publisher Link](#)]
- [10] Kenneth R. Bell et al., “Proven Success for Driven Pile Foundations,” *Deep Foundations 2002: An International Perspective on Theory, Design, Construction, and Performance*, pp. 1029-1037, 2002. [[CrossRef](#)] [[Google Scholar](#)] [[Publisher Link](#)]
- [11] Yunpeng Zhang et al., “A Novel Soil-Pile Interaction Model for Vertical Pile Settlement Prediction,” *Applied Mathematical Modelling*, vol. 99, pp. 478-496, 2021. [[CrossRef](#)] [[Google Scholar](#)] [[Publisher Link](#)]
- [12] O.A. Arab et al., “Numerical Modelling Observations of Settlement for Pad Footings Supported on Soft Clay Soil,” *IOP Conference Series: Materials Science and Engineering: The 3<sup>rd</sup> Global Congress on Construction, Material and Structural Engineering*, vol. 1200, pp. 1-9, 2021. [[CrossRef](#)] [[Google Scholar](#)] [[Publisher Link](#)]
- [13] S. Prasanth, and N. Sankar, “Prediction of Settlement of Shallow Footings on Granular Soils Using Genetic Algorithm,” *Asian Journal of Engineering and Technology*, vol. 3, no. 4, pp. 376-383, 2015. [[Google Scholar](#)] [[Publisher Link](#)]
- [14] Braja M. Das, *Principles of Foundation Engineering*, 10<sup>th</sup> ed., pp. 1-960, 2024. [[Google Scholar](#)] [[Publisher Link](#)]
- [15] Wei Dong Guo, “Visco-Elastic Load Transfer Models for Axially Loaded Piles,” *International Journal for Numerical and Analytical Methods in Geomechanics*, vol. 24, no. 2, pp. 135-163, 2000. [[CrossRef](#)] [[Google Scholar](#)] [[Publisher Link](#)]
- [16] Xiao-Mi Li, Qian-Qing Zhang, and Shan-Wei Liu, “Semianalytical Solution for Long-Term Settlement of a Single Pile Embedded in Fractional Derivative Viscoelastic Soils,” *International Journal of Geomechanics*, vol. 21, no. 2, 2021. [[CrossRef](#)] [[Google Scholar](#)] [[Publisher Link](#)]
- [17] Chun Yan Zhao, Wu Ming Leng, and Guo Yong Zheng, “Calculation and Analysis for the Time-Dependency of Settlement of the Single-Driven Pile in Double-Layered Soft Clay,” *Applied Clay Science*, vol. 79, pp. 8-12, 2013. [[CrossRef](#)] [[Google Scholar](#)] [[Publisher Link](#)]
- [18] Qibiao Wang et al., “Database Analysis of Long-Term Settlement Behavior of Pile Foundations in Shanghai Soft Coastal Clays,” *Buildings*, vol. 14, no. 11, pp. 1-23, 2024. [[CrossRef](#)] [[Google Scholar](#)] [[Publisher Link](#)]
- [19] Koichiro Danno, and Makoto Kimura, “Evaluation of Long-Term Displacements of Pile Foundation Using Coupled Fem and Centrifuge Model Test,” *Soils and Foundations*, vol. 49, no. 6, pp. 941-958, 2009. [[CrossRef](#)] [[Google Scholar](#)] [[Publisher Link](#)]
- [20] Anumita Mishra, and Nihar Ranjan Patra, “Analysis of Creep Settlement of Pile Groups in Linear Viscoelastic Soil,” *International Journal for Numerical and Analytical Methods in Geomechanics*, vol. 43, no. 14, pp. 2288-2304, 2019. [[CrossRef](#)] [[Google Scholar](#)] [[Publisher Link](#)]
- [21] E.G. Psaroudakis, G.E. Mylonakis, and N.S. Klimis, “Non-Linear Analysis of Axially Loaded Piles Using “t-z” and “q-z” Curves,” *Geotechnical and Geological Engineering*, vol. 37, pp. 2293-2302, 2019. [[CrossRef](#)] [[Google Scholar](#)] [[Publisher Link](#)]
- [22] Thejesh Kumar Garala, “The Millennium Tower: Leaning Tower of San Francisco,” *Indian Geotechnical Society*, vol. 48, no. 4, pp. 1-3, 2017. [[Publisher Link](#)]
- [23] Jonathan P. Stewart et al., “Foundation Settlement and Tilt of Millennium Tower in San Francisco, California,” *Journal of Geotechnical and Geoenvironmental Engineering*, vol. 149, no. 6, pp. 1-22, 2023. [[CrossRef](#)] [[Google Scholar](#)] [[Publisher Link](#)]
- [24] Zhen-ya Li et al., “A New Approach for Time Effect Analysis in the Settlement of Single Pile in Nonlinear Viscoelastic Soil Deposits,” *Journal of Zhejiang University SCIENCE A*, vol. 16, no. 8, pp. 630-643, 2015. [[Google Scholar](#)] [[Publisher Link](#)]
- [25] Roberto Cairo, and Enrico Conte, “Settlement Analysis of Pile Groups in Layered Soils,” *Canadian Geotechnical Journal*, vol. 43, no. 8, pp. 788-801, 2006. [[CrossRef](#)] [[Google Scholar](#)] [[Publisher Link](#)]
- [26] Mohamed A. Sakr et al., “Improvement of Soft Clay Soil with Different Techniques – State of the Art,” *International Journal of Advances in Structural and Geotechnical Engineering*, vol. 6, no. 3, pp. 35-44, 2022. [[CrossRef](#)] [[Google Scholar](#)] [[Publisher Link](#)]
- [27] Murat Ornek et al., “Numerical Analysis of Circular Footings on Natural Clay Stabilized with a Granular Fill,” *Acta Geotechnica Slovenica*, vol. 9, no. 1, pp. 61-75, 2012. [[Google Scholar](#)]
- [28] A.B. Salahudeen, and Ja'afar Abubakar Sadeeq, “Evaluation of Bearing Capacity and Settlement of Foundations,” *Leonardo Electronic Journal of Practices and Technologies*, vol. 29, pp. 93-114, 2016. [[Google Scholar](#)]
- [29] A.B. Salahudeen, and J.A. Sadeeq, “Investigation of Shallow Foundation Soil Bearing Capacity and Settlement Characteristics of Minna City Centre Development Site Using Plaxis 2d Software and Empirical Formulations,” *Nigerian Journal of Technology*, vol. 36, no. 3, pp. 663-670, 2017. [[CrossRef](#)] [[Google Scholar](#)] [[Publisher Link](#)]
- [30] Zong-Jun Sun et al., “Sensitivity Analysis of Influencing Factors of Pile Foundation Stability Based on Field Experiment,” *Structures*, vol. 54, pp. 14-22, 2023. [[CrossRef](#)] [[Google Scholar](#)] [[Publisher Link](#)]
- [31] Lilin Wang, Xin Zhao, and Shehong Liu, “A Study of Differential Foundation Settlement of Piled Raft and its Effect on the Long-Term Vertical Shortening of Super-Tall Buildings,” *Structural Design Tall Build*, vol. 30, no. 4, pp. 1-19, 2020. [[CrossRef](#)] [[Google Scholar](#)] [[Publisher Link](#)]

- [32] A. Ganal, and O. Reul, “Back Analysis of Long-Term Measurements of a High-Rise Building Founded on a Raft Foundation in Overconsolidated Clay,” *Proceedings 10<sup>th</sup> NUMGE 2023 10<sup>th</sup> European Conference on Numerical Methods in Geotechnical Engineering*, London, UK, pp. 1-6, 2023. [[CrossRef](#)] [[Google Scholar](#)] [[Publisher Link](#)]
- [33] M.C. McVay et al., “*Pile Friction Freeze: A Field and Laboratory Study. Volume 1 of 2*,” Research Center, Florida Department of Transportation, Technical Report, pp. 1-656, 1999. [[Google Scholar](#)] [[Publisher Link](#)]
- [34] Michael C. McVay, *Pile Friction Freeze: A Field and Laboratory Study*, University of Florida, vol. 2, 1999. [[Publisher Link](#)]
- [35] Albana Arreza, “*Validation of Embedded Beam Row for Anchor Modeling in PLAXIS 2D*,” Master's Thesis, Graz University of Technology, pp. 1-83, 2018. [[Publisher Link](#)]
- [36] P Manual, *PLAXIS 2D-Reference Manual*, 2020. [[Google Scholar](#)]
- [37] Queen Arista Rosmania Putri Sumarsono, As'ad Munawir, and Harimurti, “Comparative Analysis of Single Pile with Embedded Beam Row and Volume Pile Modeling under Seismic Load,” *Studia Geotechnica et Mechanica*, vol. 45, no. 1, pp. 28-40, 2023. [[CrossRef](#)] [[Google Scholar](#)] [[Publisher Link](#)]
- [38] Ben Van Der Kwaak, “*Modelling of Dynamic Pile Behaviour during an Earthquake Using PLAXIS 2D: Embedded Beam (Rows)*,” Master Thesis, Delft University of Technology, pp. 1-124, 2015. [[Publisher Link](#)]
- [39] B.A. Al-Dawoodi, M.Q. Waheed, and F.H. Rahil, “Numerical Modeling of Shallow Foundation Behavior Using Soft Soil Model,” *IOP Conference Series: Earth and Environmental Science: 2<sup>nd</sup> International Conference of Al-Esraa University College for Engineering Sciences*, Baghdad, Iraq, vol. 961, no. 1, pp. 1-11, 2022. [[CrossRef](#)] [[Google Scholar](#)] [[Publisher Link](#)]
- [40] Minna Karstunen, and Amardeep Amavasai, “*BEST SOIL: Soft Soil Modelling and Parameter Determination*,” Chalmers University of Technology, Sweden, Report, pp. 1-84, 2017. [[Google Scholar](#)] [[Publisher Link](#)]
- [41] Plaxis, *Material Models Manual 2D*, Sipilpedia, 2024. [Online]. Available: <https://sipilpedia.com/plaxis-2d-2024-2-2d-3-material-models-manual/>
- [42] J.F. Rodríguez-Rebolledo, G.Y. Auvinet-Guichard, and H.E. Martínez-Carvajal, “Settlement Analysis of Friction Piles in Consolidating Soft Soils,” *DYNA*, vol. 82, no. 192, pp. 211-220, 2015. [[CrossRef](#)] [[Google Scholar](#)] [[Publisher Link](#)]
- [43] N. Barounis, and J. Philpot, *Estimation of in-Situ Water Content and Void ratio Using CPT for Saturated Sands*, Cone Penetration Testing 2018, 1<sup>st</sup> ed., CRC Press, pp. 1-7, 2018. [[Google Scholar](#)] [[Publisher Link](#)]
- [44] Mohammad Amin Hosseini, and Mohammad Rayhani, “Evolution of Pile Shaft Capacity Over Time in Marine Soils,” *International Journal of Geo-Engineering*, vol. 8, pp. 1-15, 2017. [[CrossRef](#)] [[Google Scholar](#)] [[Publisher Link](#)]
- [45] Song Jiang et al., “Theoretical Solution for Long-Term Settlement of a Large Step-Tapered Hollow Pile in Karst Topography,” *International Journal of Geomechanics*, vol. 21, no. 8, pp. 1-14, 2021. [[CrossRef](#)] [[Google Scholar](#)] [[Publisher Link](#)]
- [46] Timothy O. Hodson, “Root-Mean-Square Error (RMSE) or Mean Absolute Error (MAE): when to Use them or Not,” *Geoscientific Model Development*, vol. 15, no. 14, pp. 5481-5487, 2022. [[CrossRef](#)] [[Google Scholar](#)] [[Publisher Link](#)]
- [47] Steve Pischke, *Ec524: Empirical Methods in Applied Economics*, 2007. [Online]. Available: <https://econ.lse.ac.uk/staff/spischke/ec524/>
- [48] S.D. Springate, “The Effect of Sample Size and Bias on the Reliability of Estimates of Error: A Comparative Study of Dahlberg's Formula,” *European Journal of Orthodontics*, vol. 34, no. 2, pp. 158-163, 2012. [[CrossRef](#)] [[Google Scholar](#)] [[Publisher Link](#)]
- [49] Miloš Marjanović et al., “Modeling of Laterally Loaded Piles Using Embedded Beam Elements,” *Proceedings of the 4<sup>th</sup> International Conference on Modern Achievements in Civil Engineering*, vol. 32, pp. 349-358, 2016. [[Google Scholar](#)] [[Publisher Link](#)]
- [50] J. Sluis et al., “Validation and Application of the Embedded Pile Row-Feature in PLAXIS 2D,” *Plaxis Bulletin*, vol. 34, pp. 10-13, 2013. [[Google Scholar](#)]
- [51] J.J. Sluis, F. Besseling, and P. Stuurwold, *Modelling of a Pile Row in a 2D Plane Strain FE-Analysis*, Numerical Methods in Geotechnical Engineering, CRC Press, pp. 277-282, 2014. [[Google Scholar](#)] [[Publisher Link](#)]
- [52] Carla M. Smulders, Saman Hosseini, and Ronald B.J. Brinkgreve, “Improved Embedded Beam with Interaction Surface,” *17<sup>th</sup> European Conference on Soil Mechanics and Geotechnical Engineering*, Reykjavik Iceland, pp. 1-6, 2019. [[Google Scholar](#)] [[Publisher Link](#)]
- [53] Yao Shan et al., “Long-Term in-Situ Monitoring on Foundation Settlement and Service Performance of a Novel Pile-Plank-Supported Ballastless Tram Track in Soft Soil Regions,” *Transportation Geotechnics*, vol. 36, 2022. [[CrossRef](#)] [[Google Scholar](#)] [[Publisher Link](#)]
- [54] Wei-Kang Lin et al., “Numerical Analysis of Pile-Supported Reinforced Embankments in Deep Soft Soil Regions Based on Soft Soil Creep Parameter Optimization,” *Advances in Civil Engineering*, vol. 2025, no. 1, pp. 1-13, 2025. [[CrossRef](#)] [[Google Scholar](#)] [[Publisher Link](#)]
- [55] Qiongyi Wang et al., “Sensitivity Analysis of Counterweight Double-Row Pile Deformation to Weak Stratum Parameters,” *Scientific Reports*, vol. 13, pp. 1-14, 2023. [[CrossRef](#)] [[Google Scholar](#)] [[Publisher Link](#)]
- [56] Y. Xu, L.M. Zhang, and W.H. Tang, “Sensitivity Analysis of Settlement of Single Piles,” *Foundation Analysis and Design: Innovative Methods*, pp. 35-41, 2012. [[CrossRef](#)] [[Google Scholar](#)] [[Publisher Link](#)]
- [57] P.J. Vardanega et al., “Sensitivity of Simplified Pile Settlement Calculations to Parameter Variation in Stiff Clay,” *Geotechnical Engineering for Infrastructure and Development: Proceedings XVI European Conference on Soil Mechanics and Geotechnical Engineering*, pp. 3777-3782, 2015. [[Google Scholar](#)] [[Publisher Link](#)]